Dynamical models of circumstellar dust shells around Long-period Variables: Spectrum, lightcurves, intensity profiles, and visibilities of IRC +10216

J.M. WINTERS[1], A.J. FLEISCHER[1], A. GAUGER[2], E. SEDLMAYR[1]

[1]Institut für Astronomie & Astrophysik, TU Berlin, FRG
[2]Los Alamos National Laboratory, Group T–4, New Mexico, USA

Poster paper presented at IAU Symposium 170:
CO: Twenty–five Years of Millimeter–wave Spectroscopy
29 May – 2 June 1995 Tucson, Arizona

1 Introduction

Observations of Long–period variables (LPVs) show several rather complex characteristics, which are by now not very well understood. These comprise for example

- non–sinusodial *lightcurves*, showing a drift in time either of the average magnitude or of the amplitude (e.g. Le Bertre 1992)
- pronounced internal structures in the *spatial spectra* (visibilities) of the circumstellar shells (e.g. Ridgway & Keady 1988, Danchi et al. 1994)
- step–like structures in the *brightness profile* on a spatial scale of a few stellar radii at least in the case of IRC +10216 (Richichi 1993).

The observations also indicate that a considerable amount of dust is present in the circumstellar shells of most LPVs.

To arrive at a reliable physical description of circumstellar dust shells (CDS) around LPVs one has to consider the complex interplay among hydrodynamics, thermodynamics, and formation, growth, and evaporation of dust grains.

The consistent treatment of these interactions leads to a number of dynamical effects, e.g.

- a discrete, shell–like radial distribution of dust (Fleischer et al. 1992)
- dust accelerated shocks (Fleischer et al. 1992)
- a multiperiodic temporal behavior of the CDS (Fleischer et al. 1995a,b)

which strongly influence the optical appearance of these models (Winters et al. 1994b, 1995).

In this poster, we present these effects for one hydrodynamical model which is capable of explaining several different observations of the prominent carbon star IRC +10216.

2 Method

2.1 Hydrodynamics (Details see Fleischer et al. 1992)

- 1–D Lagrangian code in spherical symmetry,
- *simultaneous* solution of
  hydrodynamics, (equilibrium) chemistry,
  dust formation, –growth, and –evaporation (Gauger et al. 1990),
  (grey, semianalytical) radiative transfer (Lucy, 1971, 1976)

=> atmospheric structure at time t

2.2 Radiative transfer (Details see Winters et al. 1994a)

- radiative transfer equation in spherical geometry, Feautrier–type iteration between moment equations and formal solution
- radiative transfer processes:

  gas: grey absorption and thermal emission

  dust: frequency dependent absorption and thermal emission,
  opacity calculated from the small particle limit of Mie theory,
  spherical grains are assumed,
  optical properties of amorphous carbon, described by the complex refractive index given in Preibisch et al. 1993

=> angle and frequency dependent radiation field at time t

3.1 Model parameters

Due to the consistent treatment of the dynamical dust shell problem, our models are completely determined by specifying *6* parameters. The model for IRC +10216 presented here is determined by:

stellar mass	M_*	=	$1 M_\odot$
stellar temperature	T_*	=	2500 K
stellar luminosity	$L_*(t=0)$	=	$2.4\,10^4 L_\odot$
carbon–to–oxygen ratio	$\epsilon_{\rm C}/\epsilon_{\rm O}$	=	1.20
pulsation period	P	=	650 d
piston amplitude	$\Delta u_{\rm P}$	=	6 km/s

3.2 Resulting quantities

This model yields values for the final outflow velocity, the mass loss rate, and the dust–to–gas ratio by mass of

average outflow velocity	$< v_\infty >$	=	14.3 km/s
observation	13.7 . . . 14.8 (Olofsson et al. 1993)		
average mass loss rate	$< \dot{M} >$	=	$1.2\,10^{-4} M_\odot$/yr
observation	$\approx 5\,10^{-5}$ (Knapp & Morris 1985)		
average dust–to–gas mass ratio	$< \rho_{\rm d}/\rho_{\rm g} >$	=	$8.1\,10^{-4}$
observation	$\approx 1.3\,10^{-3}$ (Knapp 1985)		

4 Results

- Resulting values of the outflow velocity, the mass loss rate, and the dust–to–gas mass ratio are in reasonable agreement with the respective values derived from observations of IRC +10216 (cf. 3.2)
- Observed spectrum at minimum and maximum phase of the lightcurve is well reproduced by the synthetic energy distribution obtained at the respective phases from the model calculation. *We derive a distance to IRC +10216 of* $d = 170$ *pc* (cf. Fig. 1)
- Spatial structure of the dust shell model is not recovered each pulsation cycle, but only after approximately 4 pulsation periods. => *The dust shell possesses its own intrinsic timescale* (cf. Figs. 2 and 4). Synthetic brightness profiles at longer wavelengths show a step–like structure on a spatial scale of a few stellar radii. Synthetic visibilities show a rippled internal structure at longer wavelengths (cf. Fig. 2)
- Spatial spectra observed at different wavelengths near maximum phase of the lightcurve are satisfactorily reproduced by the synthetic visibilities obtained at a respective phase of the model calculation (open triangles at $t \approx 10.7\,$P in Fig. 4), assuming the distance of 170 pc derived from the energy distribution (cf. Fig. 3)

- Synthetic *lightcurves show a multiperiodic behavior* in agreement with the trend observed at different wavelengths over 3 periods (cf. Fig. 4). In particular, *the temporal evolution of the minima, which is different at short and long wavelengths is correctly reproduced by the model calculation*

- *Observed brightness profile of IRC +10216 at* 1.65μm *is well reproduced by the synthetic profile, assuming a distance of 170 pc* (cf. Fig. 5)

References:

Danchi W. C., Bester M., Degiacomi C. G., Greenhill L. J., Townes C. H., 1994, *AJ* 107, 1469
Fleischer A. J., Gauger A., Sedlmayr E., 1992, *A&A* 266, 321
Fleischer A. J., Gauger A., Sedlmayr E., 1995, *A&A* 297, 543
Fleischer A. J., Winters J. M., Gauger A., Sedlmayr E., 1995, In *CO: Twenty-five Years of Millimeter-wave Spectroscopy*, Kluwer Academic Publishers, **in press**
Gauger A., Gail H.-P., Sedlmayr E., 1990, *A&A* 235, 345
Knapp G. R., 1985, *ApJ* 293, 273
Knapp G. R., Morris M., 1985, *ApJ* 292, 640
Le Bertre T., 1992, *A&AS* 94, 377
Lucy L. B., 1971, *ApJ* 163, 95
Lucy L. B., 1976, *ApJ* 205, 482
Olofsson H., Eriksson K., Gustafsson B., Carlström U., 1993, *ApJS* 87, 267
Preibisch T., Ossenkopf V., Yorke H. W., Henning T., 1993, *A&A* 279, 577
Richichi A., 1993, private communication
Ridgway S. T., Keady J. J., 1988, *ApJ* 326, 843
Winters J. M., Dominik C., Sedlmayr E., 1994a, *A&A* 288, 255
Winters J. M., Fleischer A. J., Gauger A., Sedlmayr E., 1994b, *A&A* 290, 623
Winters J. M., Fleischer A. J., Gauger A., Sedlmayr E., 1995, *A&A* in press

Acknowledgements: This work has been supported by the BMBF (Grant 2BT12A), the DFG (Grant Se 420/8-1), and the DOE. The calculations were performed on the CRAY–computers of the ZIB (Berlin).

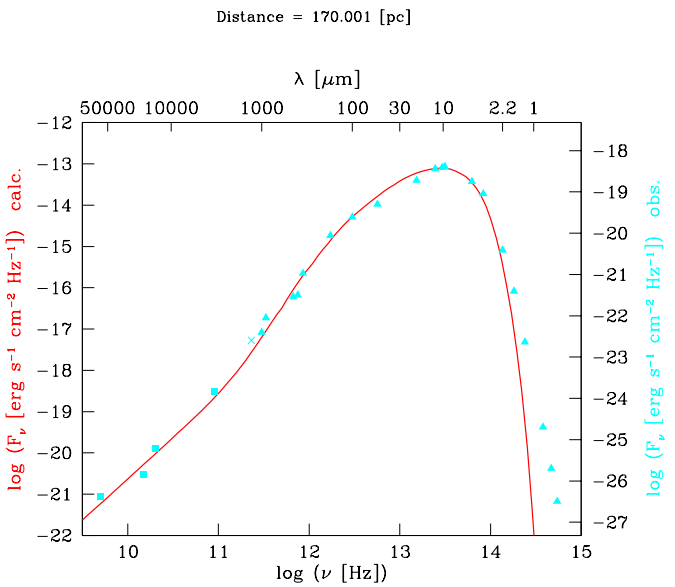

Figure 1: a) Observed spectrum of IRC +10216 at **maximum** phase of the lightcurve (blue symbols) and theoretical spectrum of the dust shell model (red solid line) at $t = 14.60P$, cf. Fig. 4.

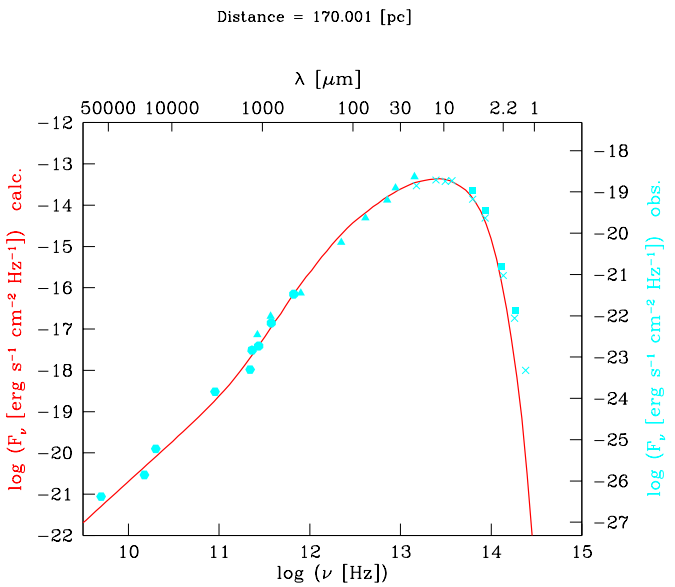

Figure 1: b) Observed spectrum of IRC +10216 at **minimum** phase of the lightcurve (blue symbols) and theoretical spectrum of the dust shell model (red solid line) at $t = 13.90P$, cf. Fig. 4.

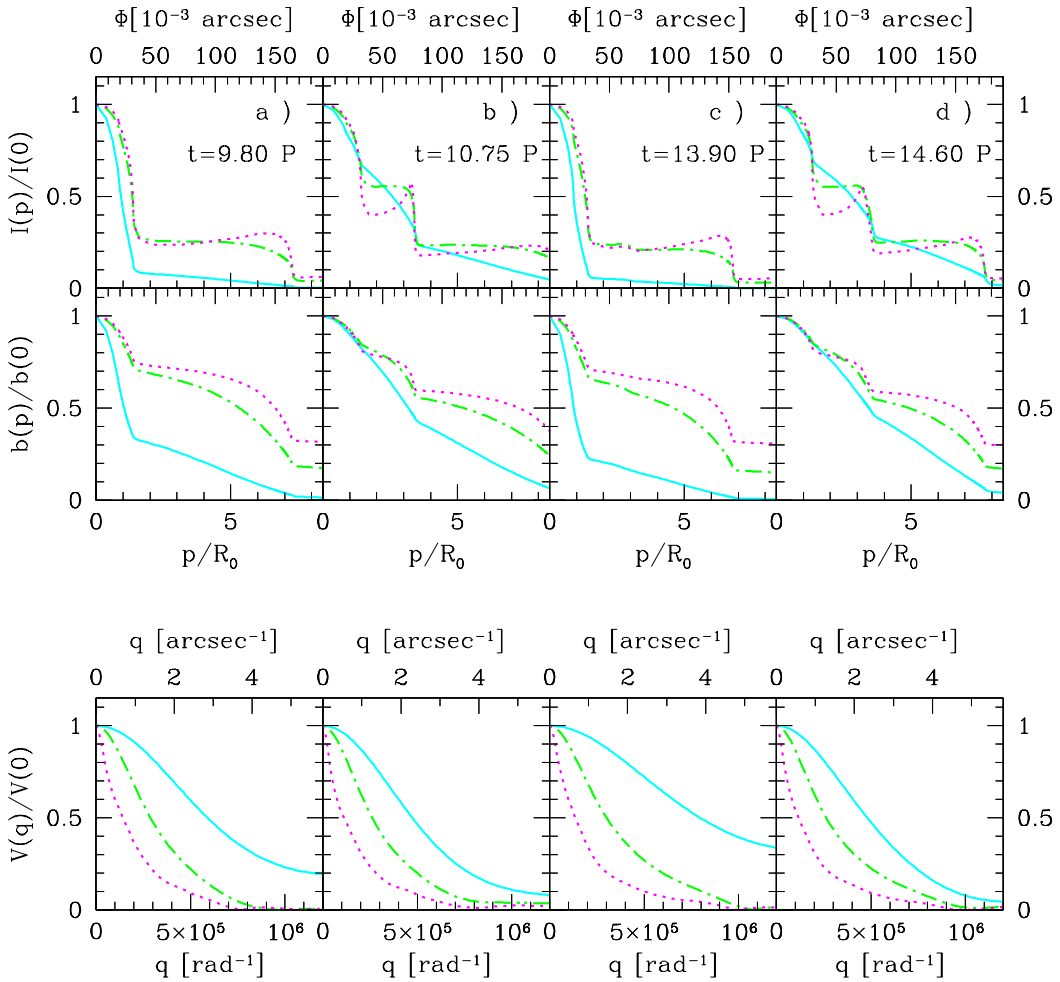

Figure 2: Intensity profiles (upper diagrams), integrated brightness distributions (second row), and visibilities (lower panel) of the dust shell model for $\lambda = 1.5\mu$m (solid blue lines), $\lambda = 5\mu$m (dash–dotted green lines), and $\lambda = 12\mu$m (dotted red lines) at different instants of time (cf. Fig. 4.). A distance of $d = 170\,$pc is assumed.

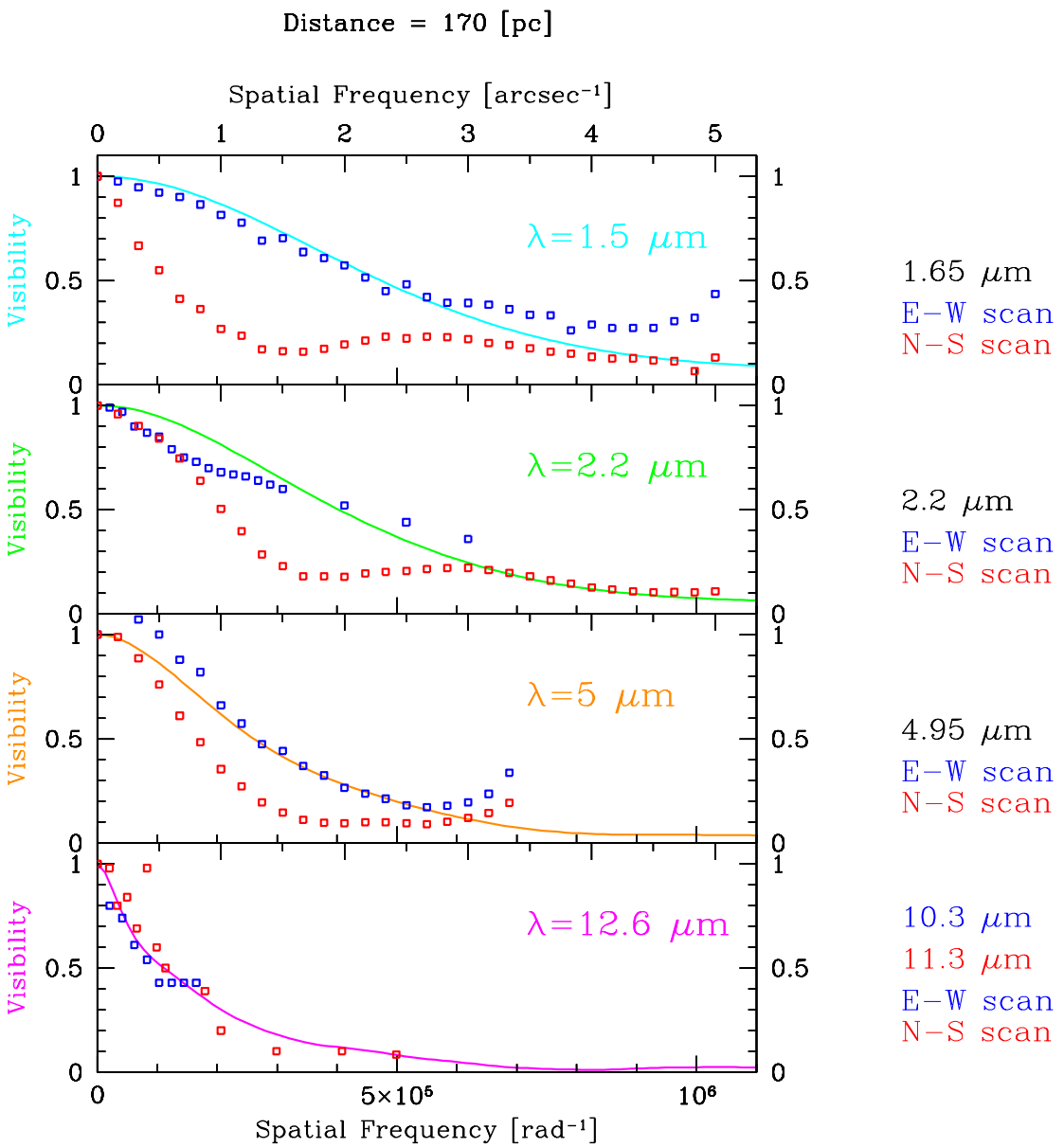

Figure 3: Observed visibilities of IRC +10216 around **maximum** phase of the lightcurve (blue and red symbols, after Ridgway & Keady (1988)) and theoretical visibilities of the dust shell model (solid lines) at $t = 10.75P$, cf. Fig. 4.

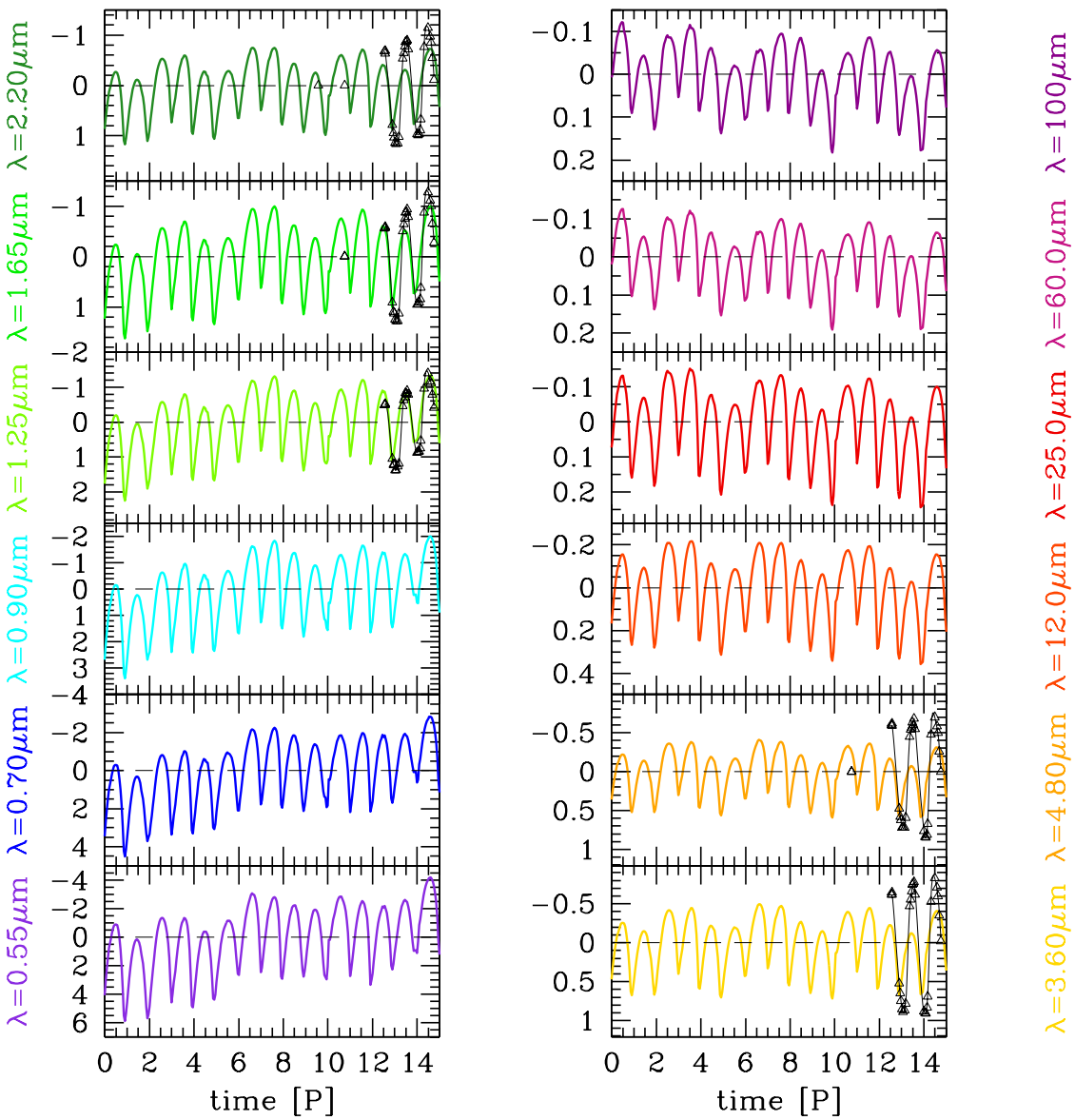

Figure 4: Observed lightcurves of IRC +10216 (black symbols at $\lambda = 1.25\mu$m (J), $\lambda = 1.65\mu$m (H), $\lambda = 2.20\mu$m (K), $\lambda = 3.60\mu$m (L), $\lambda = 4.80\mu$m (M) (Le Bertre 1992) and theoretical lightcurves of the dust shell model (solid lines) at different wavelengths over a time interval of 15 pulsation periods. The lightcurves are plotted in magnitudes normalized to the mean magnitude. Note the different scaling of the ordinate at different wavelengths.

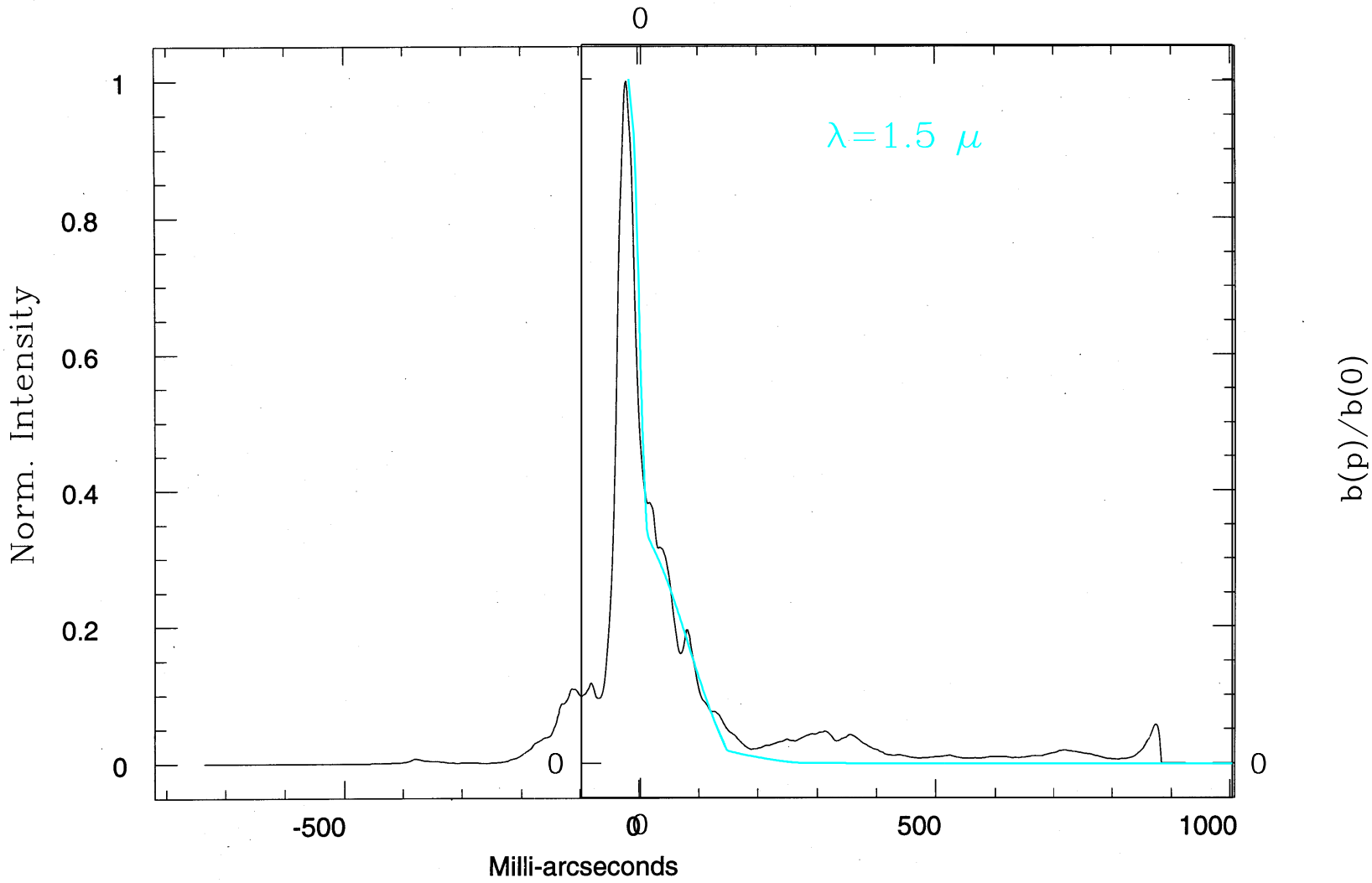

Figure 5: Observed radial brightness profile of IRC +10216 at $\lambda = 1.65\mu$m, reconstructed from a lunar occultation lightcurve (black solid line, this figure was kindly made available to us by Dr. A. Richichi) and synthetic brightness profile at $\lambda = 1.54\mu$m of the dust shell model (blue solid line) at $t = 9.80P$, cf. Fig. 4.